

NACA TN 1984

# NATIONAL ADVISORY COMMITTEE FOR AERONAUTICS

TECHNICAL NOTE 1984

A SEMIEMPIRICAL METHOD FOR ESTIMATING THE ROLLING  
MOMENT DUE TO YAWING OF AIRPLANES

By John P. Campbell and Alex Goodman

Langley Aeronautical Laboratory  
Langley Air Force Base, Va.

PROFESSOR AIRCHILD  
ENGINEERING LIBRARY



Washington  
December 1949

NATIONAL ADVISORY COMMITTEE FOR AERONAUTICS

TECHNICAL NOTE 1984

A SEMIEMPIRICAL METHOD FOR ESTIMATING THE ROLLING  
MOMENT DUE TO YAWING OF AIRPLANES

By John P. Campbell and Alex Goodman

SUMMARY

A method is presented for estimating the rolling moment due to yawing of airplanes. The results are given in terms of the derivative  $C_{l_r}$ , which is defined as the rate of change of rolling-moment coefficient with yawing-velocity parameter. The method is semiempirical in that it provides for experimentally determined correction factors to be applied to the theory. The correction factor for the wing is the incremental value of the rolling moment due to sideslip  $C_{l_\beta}$  obtained by subtracting the experimental value of  $C_{l_\beta}$  from the theoretical value. This incremental value of  $C_{l_\beta}$ , which is expressed in radians, is added to the theoretical value of  $C_{l_r}$  to give the corrected value of  $C_{l_r}$  for the wing. Similar use is made of experimental data to estimate the contribution of the vertical tail to  $C_{l_r}$ .

Comparisons of experimental and estimated values of  $C_{l_r}$  for 22 different wing configurations and 8 complete models indicate that this method provides a substantial improvement over existing theoretical methods for estimating  $C_{l_r}$ .

INTRODUCTION

Comparisons of theoretically and experimentally determined values of the rate of change of the rolling-moment coefficient with the yawing-velocity parameter  $C_{l_r}$  (referred to as the rolling moment due,

to yawing) have indicated that the theory of reference 1 is inadequate for estimating  $C_{l_r}$ , especially in the case of swept wings. (See references 1 and 2.) The largest discrepancies between theory and experiment occur at moderate and high lift coefficients and are attributed to the fact that the theory is based on potential-flow concepts and thus does not account for the partial flow separation which usually exists on swept wings even at moderate angles of attack. A study has therefore been made to find a method of estimating  $C_{l_r}$  which does take into account this partial flow separation. In one promising method found in this study, use is made of the similarity between  $C_{l_r}$  and the derivative  $C_{l_\beta}$ , the rolling moment due to sideslip. A description of the method and a comparison of experimental values of  $C_{l_r}$  and values estimated by this method are given in the present paper.

The method of estimating  $C_{l_r}$  presented herein is semiempirical in that it necessitates an experimentally determined correction factor to be applied to theory. The correction factor for the wing is merely the incremental value of  $C_{l_\beta}$  obtained by subtracting the experimental value of  $C_{l_\beta}$  from the theoretical value (reference 1) for the given wing at the same lift coefficient. This incremental value of  $C_{l_\beta}$ , expressed in radians, is then added to the theoretical value of  $C_{l_r}$  obtained from reference 1 to give the corrected value of  $C_{l_r}$  for the wing. Similar use is made of experimental data to estimate the tail contribution to  $C_{l_r}$ .

One advantage of this method is that lateral-stability force-test data are usually available for obtaining the experimental values of  $C_{l_\beta}$  for the particular airplane under consideration. Another advantage is that the correction factor can be based on an experimental value of  $C_{l_\beta}$  obtained from force tests made at much higher values of Reynolds number and Mach number than can be reached with existing equipment for measuring  $C_{l_r}$ .

## SYMBOLS

The symbols used in the analysis and in the presentation of the results are defined herein. The data presented are referred in all cases to the stability system of axes.

$$C_L \quad \text{lift coefficient} \left( \frac{\text{Lift}}{\frac{1}{2}\rho V^2 S} \right)$$

$$C_l \quad \text{rolling-moment coefficient} \left( \frac{\text{Rolling moment}}{\frac{1}{2}\rho V^2 S b} \right)$$

$$C_Y \quad \text{lateral-force coefficient} \left( \frac{\text{Lateral force}}{\frac{1}{2}\rho V^2 S} \right)$$

$$C_{l_r} = \frac{\partial C_l}{\partial \frac{r b}{2V}}$$

$$C_{l_\beta} = \frac{\partial C_l}{\partial \beta}$$

$$C_{Y_\beta} = \frac{\partial C_Y}{\partial \beta}$$

$\rho$  mass density of air, slugs per cubic foot

$S$  wing area, square feet

$V$  airspeed, feet per second

$\bar{c}$  wing mean chord, feet ( $b/A$ )

$b$  wing span, feet

$\bar{x}$  longitudinal distance rearward from airplane center of gravity to wing aerodynamic center, feet

l	longitudinal distance rearward from center of gravity to center of pressure of vertical tail, measured parallel to longitudinal stability axis, feet
z	vertical distance upward from center of gravity to center of pressure of vertical tail measured perpendicular to longitudinal stability axis, feet
$\Lambda$	sweep angle of wing quarter chord line (positive for sweepback), degrees
A	aspect ratio ( $b^2/S$ )
$\frac{rb}{2V}$	yawing-velocity parameter
r	yawing angular velocity, radians per second
$\alpha$	angle of attack, degrees
$\beta$	angle of sideslip, radians
$a_0$	section-lift-curve slope, radians
$\lambda$	taper ratio $\left( \frac{\text{Tip chord}}{\text{Root chord}} \right)$
$\Gamma$	dihedral angle, degrees

#### ANALYSIS AND METHOD

##### Contribution of Wing to $C_{l_r}$

Analysis of the experimental data presented in references 1 and 2 and of similar data from other investigations conducted by the NACA indicates that the discrepancies between theoretical and experimental values of  $C_{l_r}$  for wings are quite similar to the discrepancies between theoretical and experimental values of  $C_{l_\beta}$ . Typical data which illustrate this point are presented in figure 1. For both  $C_{l_r}$  and  $C_{l_\beta}$  only moderate disagreements between theory and experiment exist at low lift coefficients, but very large disagreements usually

occur at the higher lift coefficients for swept wings. As stated previously, the large difference between theory and experiment at moderate and high lift coefficients for swept wings is probably caused by partial flow separation over the wing that is not accounted for by theory.

The observed similarity between  $C_{l_r}$  and  $C_{l_\beta}$  of the wing, regarding the comparison of theory and experiment, is approximately expressed by the equation

$$C_{l_{r_{\text{exp}}}} - C_L \left( \frac{C_{l_r}}{C_L} \right)_{\text{theory}} = - C_{l_{\beta_{\text{exp}}}} + C_L \left( \frac{C_{l_\beta}}{C_L} \right)_{\text{theory}} \quad (1)$$

where both  $C_{l_r}$  and  $C_{l_\beta}$  are expressed in terms of radians.

Rearranging this expression gives the following equation for estimating the contribution of the wing to  $C_{l_r}$

$$C_{l_{r_{\text{wing}}}} = C_L \left( \frac{C_{l_r}}{C_L} \right)_{\text{theory}} + C_L \left( \frac{C_{l_\beta}}{C_L} \right)_{\text{theory}} - C_{l_{\beta_{\text{exp}}}} \quad (2)$$

The experimental value of  $C_{l_\beta}$  can be obtained from lateral-stability force-test data for the wing under consideration. Theoretical values of  $C_{l_r}/C_L$  and  $C_{l_\beta}/C_L$  can be obtained from the formulas and charts of reference 1. For convenience, two of the estimation charts of reference 1 for a taper ratio of 1.0 are presented in figures 2 and 3 of the present paper. Values of  $C_{l_r}/C_L$  and  $C_{l_\beta}/C_L$  for taper ratios of 0.25 and 0.50 can be calculated by the methods described in reference 1.

#### Contribution of Vertical Tail to $C_{l_r}$

In order to obtain the values of  $C_{l_r}$  for a complete airplane it is of course necessary to add the contributions of the vertical tail, fuselage, and perhaps other components to the value obtained for the wing alone. Usually the fuselage contribution is neglected and the vertical-tail contribution is assumed to be

$$\Delta C_{l_{r\text{tail}}} = -2\frac{l}{b} \frac{z}{b} \Delta C_{Y_{\beta\text{tail}}} \quad (3)$$

where  $l$ ,  $z$ , and  $b$  are determined from the geometry of the airplane and  $\Delta C_{Y_{\beta\text{tail}}}$  is obtained from lateral-stability force-test data or, if such data are not available, from conventional estimation procedures.

The contribution of the vertical tail to  $C_{l_{\beta}}$  can be estimated from a similar equation:

$$\Delta C_{l_{\beta\text{tail}}} = \frac{z}{b} \Delta C_{Y_{\beta\text{tail}}} \quad (4)$$

Dividing (3) by (4) and rearranging gives

$$\Delta C_{l_{r\text{tail}}} = -2\frac{l}{b} \Delta C_{l_{\beta\text{tail}}} \quad (5)$$

If force-test data are available for determining  $\Delta C_{l_{\beta\text{tail}}}$ , equation (5) is probably more reliable than equation (3) because it takes into account any interference effects that might cause the effective vertical location of the center of pressure of the tail to be different from the location determined from geometrical procedures.

Equation (5) indicates that if the factor  $l/b$  has a value of 0.5,  $\Delta C_{l_{r\text{tail}}}$  is equal to  $-\Delta C_{l_{\beta\text{tail}}}$ . In many cases the value of  $l/b$  is approximately 0.5, and in these cases equation (2) can be adapted to estimate the  $C_{l_r}$  of the complete airplane by using for  $C_{l_{\beta\text{exp}}}$  the experimental value of  $C_{l_{\beta}}$  for the complete airplane instead of  $C_{l_{\beta}}$  for the wing alone. For cases in which  $l/b$  is not approximately 0.5, however, equation (5) should be used to estimate the tail contribution to  $C_{l_r}$  and equation (2) the wing contribution.

## EXPERIMENTAL VERIFICATION OF METHOD

In order to check the method, experimental values of  $C_{L_r}$  for the 22 different wing configurations listed in table I and 8 complete models listed in table II have been compared with values of  $C_{L_r}$  given by equations (2) and (5). The results of the comparison are presented in figures 4 to 18. Also shown in these figures are experimental values of  $C_{L_\beta}$  and the theoretical values of  $C_{L_\beta}$  and  $C_{L_r}$  obtained from reference 1. The experimental results for the 22 wings include data which show the effects of systematic variations of aspect ratio, sweepback, and taper ratio and the effects of changes in airfoil section, flap configuration, and geometric dihedral angle. None of the complete models for which results are presented was equipped with a horizontal tail.

## Wings

The comparisons of estimated and experimental values of  $C_{L_r}$  for wings 1 to 10, which are shown in figures 4 to 8, generally indicate fair to good agreement except for the wings of aspect ratio 1.34. Even in the cases where quantitative agreement is not obtained, the trend of the variation of  $C_{L_r}$  with lift coefficient is indicated by the estimated values. A comparison of the results for wings 5 and 10 (figs. 6 and 8, respectively), which have the same plan form except that one is swept back and the other swept forward, shows that the present method satisfactorily predicts the different effect of partial flow separation over the wing in the two cases - a decrease in  $C_{L_r}$  for the sweptback wing and an increase in  $C_{L_r}$  for the sweptforward wing.

The results for wings 5, 11, 12, and 13, presented in figures 6, 9, and 10, show that the agreement between the experimental and estimated values is not quite so good for the tapered wings (wings 11, 12, and 13) as for the untapered wing (wing 5). The trends in the variation of  $C_{L_r}$ , however, are clearly shown by the estimated values. The results for wing 14, which has a taper ratio of 0, show good agreement between the estimated and experimental values of  $C_{L_r}$ . Theoretical values of  $C_{L_r}/C_L$  and  $C_{L_\beta}/C_L$  for a taper ratio of 0.25 were used in making the estimate



for wing 14 since values of  $C_{l_r}/C_L$  for a wing having a taper ratio of 0 and an aspect ratio as high as 2.31 were not available from the present theories.

The results for wings 5, 15, and 16, presented in figures 6 and 11, show that the present method (equation (2)) predicts the effects of airfoil section on the variation of  $C_{l_r}$  with lift coefficient. The estimated values are in good agreement with the measured values in showing that, as the airfoil section is changed from an NACA 0012 to an NACA 65<sub>1</sub>-012 and then to a 12-percent-thick biconvex section, the maximum value of  $C_{l_r}$  becomes progressively smaller and the departure from a linear variation of  $C_{l_r}$  with  $C_L$  occurs at progressively lower lift coefficients.

The results presented in figure 12 for the wings with dihedral (wings 17 and 18) show that although equation (2) gives values that are in fair agreement with the experimental results, the agreement is not so good as for the same wing with 0° dihedral (wing 5). The theory of reference 1 was not corrected to account for dihedral because no satisfactory theoretical method of correcting  $C_{l_r}$  for dihedral has been developed. (See reference 3.) Even though theoretical values for 0° dihedral are used, however, the present estimation method appears to account satisfactorily for the opposite effects of positive and negative dihedral on  $C_{l_r}$ .

The comparisons of experimental and estimated results for four flapped wing configurations (wings 19 to 22) are shown in figures 13 and 14. Good quantitative agreement is indicated for wings 20 and 21, whereas qualitative agreement regarding the trend of the variation of  $C_{l_r}$  with  $C_L$  is shown for the other two wings. The discrepancies at zero lift between the experimental and theoretical (reference 1) values of both  $C_{l_r}$  and  $C_{l_\beta}$  for the wings with 0.9 span split flaps (wings 20 and 22) are attributed partly to the fact that at zero lift these wings are at a negative angle of attack which (because of the sweepback) causes the wings to have effectively a positive dihedral angle. For example, the discrepancies at low lift coefficients between theory and experiment for both  $C_{l_r}$  and  $C_{l_\beta}$  are about the same for wing 20 as for wing 17 which has a dihedral angle of 10°. In the case of the wing with the 0.4 span flaps (wing 19) at zero lift, an effect opposite to that for wing 18 occurs because, even though the wing is at a negative angle of attack and therefore effectively has positive dihedral, the part of the wing outboard of the flap is producing negative lift and thus tends to give values of  $C_{l_\beta}$  and  $C_{l_r}$

opposite in sign to those obtained at positive lift coefficients. No discrepancy exists at zero lift for the wing with nose flaps (wing 21) because this wing, like the unflapped wing (wing 5), gives zero lift at zero angle of attack. For all four of the flapped wings, the discrepancies that occur at low as well as at high lift coefficients are accounted for, at least qualitatively, by equation (2).

### Complete Models

Comparisons of experimental and estimated values of  $C_{L_r}$  for the eight complete models are presented in figures 15 to 18. For the estimated values, the  $C_{L_r}$  for the vertical-tail-off condition was determined from equation (2) and the contribution of the vertical tail was determined from equation (5). Although equation (2) was intended to be used only for estimating the wing contribution, it was used in these cases to estimate the values of  $C_{L_r}$  for the wing-fuselage combination because the contribution of the fuselage is slight and is usually neglected. When equation (5) was used to estimate the tail contribution, the variation of  $l/b$  with angle of attack was taken into account.

The results for models 1 and 2 (fig. 15) indicate that equation (2) is satisfactory for estimating the wing-fuselage contribution to  $C_{L_r}$  and that equation (5) gives a satisfactory prediction of the tail contribution so that the estimates for the complete models are in fairly good agreement with the experimental data. Since models 1 and 2 are equipped with wing 14, the effect of the fuselage on  $C_{L_r}$  for these models can be ascertained by a comparison of the data of figure 10 (wing 14) with the tail-off data of figure 15. This comparison indicates that the effect of the fuselage in these cases was quite small. At zero lift coefficient, models 1 and 2 have identical values of  $C_{L_\beta}$ , but because of the different tail lengths (table II) the value of  $C_{L_r}$  for model 1 is less than half that of model 2. The good agreement between estimated and experimental values of  $C_{L_r}$  at zero lift indicate that equation (5) satisfactorily accounts for this difference in tail length.

The agreement of estimated and experimental results for model 3 (fig. 16), is not so good as for models 1 and 2. Since these three models have the same wing-fuselage combination, the poorer agreement

in the case of model 3 is apparently caused by an overestimation of the tail contribution.

In the case of model 4, which is equipped with wing 5, the agreement between the estimated and experimental values for the wing-fuselage combination (fig. 16) is not so good as the agreement in the case of the wing alone (fig. 6). The experimental data show that the addition of the fuselage caused a decrease in  $C_{l_r}$  throughout the lift range but did not appreciably affect  $C_{l_\beta}$ . This fact accounts for the disagreement in the tail-off case for model 4. Since the disagreement in the tail-on case is about the same as that for tail off, the estimate of the tail contribution appears satisfactory for this model.

The agreement between estimated and experimental values of  $C_{l_r}$  for models 5 and 6 (fig. 17) is very good over the lift range for both the tail-off and tail-on conditions. These models had the same fuselage and wing (wing 13) but had vertical tails of different size. The close agreement between estimated and experimental values for these two models is surprising in view of the disagreement indicated at the higher lift coefficients for the wing alone (wing 13, fig. 10). The data for models 5 and 6 are probably more reliable than the data for wing 13 because the model data were obtained from several tests, all of which showed similar results, whereas the wing alone data were obtained from a single test.

Results are presented in figure 18 for models 7 and 8 which have the same wing and vertical tail area as model 5 but which have different fuselage lengths and different values of  $l/b$ . The results for model 7, which has the short fuselage, show good agreement between the calculated and experimental values. In the case of the model with the long fuselage (model 8), however, the estimated values are generally higher than the experimental values for both the tail-off and tail-on conditions. As in the case of models 5 and 6, the agreement between estimated and measured values for models 7 and 8 is better than for the corresponding wing alone (wing 13) at the higher lift coefficients.

## CONCLUDING REMARKS

On the basis of the comparisons of experimental and estimated values of  $C_{l_r}$  for the 22 different wing configurations and 8 complete models, the procedure presented for estimating the rolling moment due to yawing appears to provide a substantial improvement over existing theoretical methods.

Langley Aeronautical Laboratory  
National Advisory Committee for Aeronautics  
Langley Air Force Base, Va., September 13, 1949

## REFERENCES

1. Toll, Thomas A., and Queijo, M. J.: Approximate Relations and Charts for Low-Speed Stability Derivatives of Swept Wings. NACA TN 1581, 1948.
2. Goodman, Alex, and Brewer, Jack D.: Investigation at Low Speeds of the Effect of Aspect Ratio and Sweep on Static and Yawing Stability Derivatives of Untapered Wings. NACA TN 1669, 1948.
3. Queijo, M. J., and Jaquet, Byron M.: Investigation of Effects of Geometric Dihedral on the Low-Speed Static Stability and Yawing Characteristics of an Untapered  $45^\circ$  Sweptback-Wing Model of Aspect Ratio 2.61. NACA TN 1668, 1948.

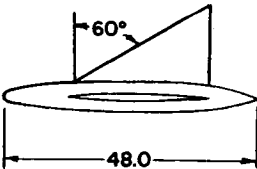
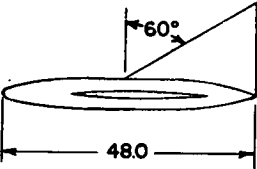
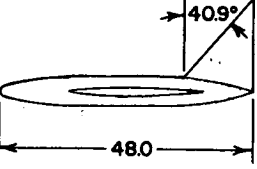
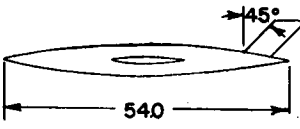
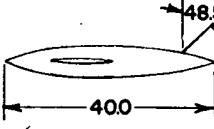
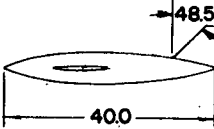
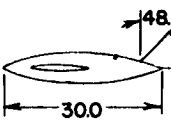
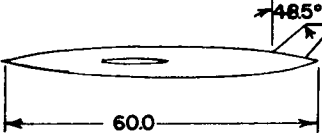
TABLE I  
SUMMARY OF PERTINENT INFORMATION REGARDING WINGS CONSIDERED IN ANALYSIS

Wing	Sweep angle, $\Lambda$ (deg)	Aspect ratio, $A$	Taper ratio, $\lambda$	Span, $b$ (ft)	Dihedral angle, $\Gamma$ (deg)	Test Reynolds number	Airfoil section	Figure	Source
1	0	1.34	1.00	2.21	0	$1.58 \times 10^6$	NACA 0012	4	Reference 2
2	45	1.34	1.00	2.20	0	1.56	NACA 0012	4	
3	60	1.34	1.00	2.21	0	1.56	NACA 0012	5	
4	0	2.61	1.00	3.08	0	1.10	NACA 0012	5	
5	45	2.61	1.00	3.05	0	1.10	NACA 0012	6	
6	60	2.61	1.00	3.05	0	1.08	NACA 0012	6	
7	0	5.16	1.00	4.26	0	.78	NACA 0012	7	
8	45	5.16	1.00	4.26	0	.77	NACA 0012	7	
9	60	5.16	1.00	4.28	0	.76	NACA 0012	8	
10	45	2.61	1.00	3.05	0	1.10	NACA 0012	8	
11	45	2.61	.50	3.05	0	1.19	NACA 0012	9	NACA tests
12	45	2.61	.25	3.05	0	1.23	NACA 0012	9	
13	45	4.00	.60	3.00	0	.71	NACA 65A008	10	
14	52.2	2.31	0	3.04	0	1.62	NACA 65(06)-006.5	10	
15	45	2.61	1.00	3.05	0	1.10	NACA 65 <sub>1</sub> -012	11	
16	45	2.61	1.00	3.05	0	1.10	12-percent biconvex	11	
17	45	2.61	1.00	3.05	10	1.10	12-percent biconvex	12	
18	45	2.61	1.00	3.05	-10	1.10	12-percent biconvex	12	
a19	45	2.61	1.00	3.05	0	1.10	NACA 0012	13	
b20	45	2.61	1.00	3.05	0	1.10	NACA 0012	13	
c21	45	2.61	1.00	3.05	0	1.10	NACA 0012	14	
d22	45	2.61	1.00	3.05	0	1.10	NACA 0012	14	



aWing with 0.4 span split flaps.  
 bWing with 0.9 span split flaps.  
 cWing with nose flaps.  
 dWing with nose and 0.9 span split flaps.

TABLE II  
SUMMARY OF PERTINENT INFORMATION REGARDING COMPLETE MODELS CONSIDERED IN ANALYSIS

Model	Side elevation (Dimensions in inches)	Wing aspect ratio	Fineness ratio of fuselage	Vertical tail aspect ratio	Tail area Wing area	$\left(\frac{l}{b}\right)_{\alpha=0^\circ}$ (d)	$\left(\frac{e}{b}\right)_{\alpha=0^\circ}$ (d)
1		<sup>a</sup> 2.31	7.38	1.15	0.500	0.144	0.167
2		<sup>a</sup> 2.31	7.38	1.15	.500	.392	.167
3		<sup>a</sup> 2.31	7.38	2.31	.250	.572	.167
4		<sup>b</sup> 2.61	8.34	1.29	.100	.576	.110
5		<sup>c</sup> 4.00	6.67	1.00	.150	.464	.089
6		<sup>c</sup> 4.00	6.67	1.00	.225	.464	.108
7		<sup>c</sup> 4.00	5.00	1.00	.150	.347	.089
8		<sup>c</sup> 4.00	10.00	1.00	.150	.697	.089

<sup>a</sup>Same wing as wing 14, table I.  
<sup>b</sup>Same wing as wing 5, table I.  
<sup>c</sup>Same wing as wing 13, table I.

<sup>d</sup>Center of pressure of the triangular vertical tails was assumed to be the center of tail area for models 1 to 3 and for the trapezoidal tails the 25-percent station of the tail mean aerodynamic chord for models 4 to 8.



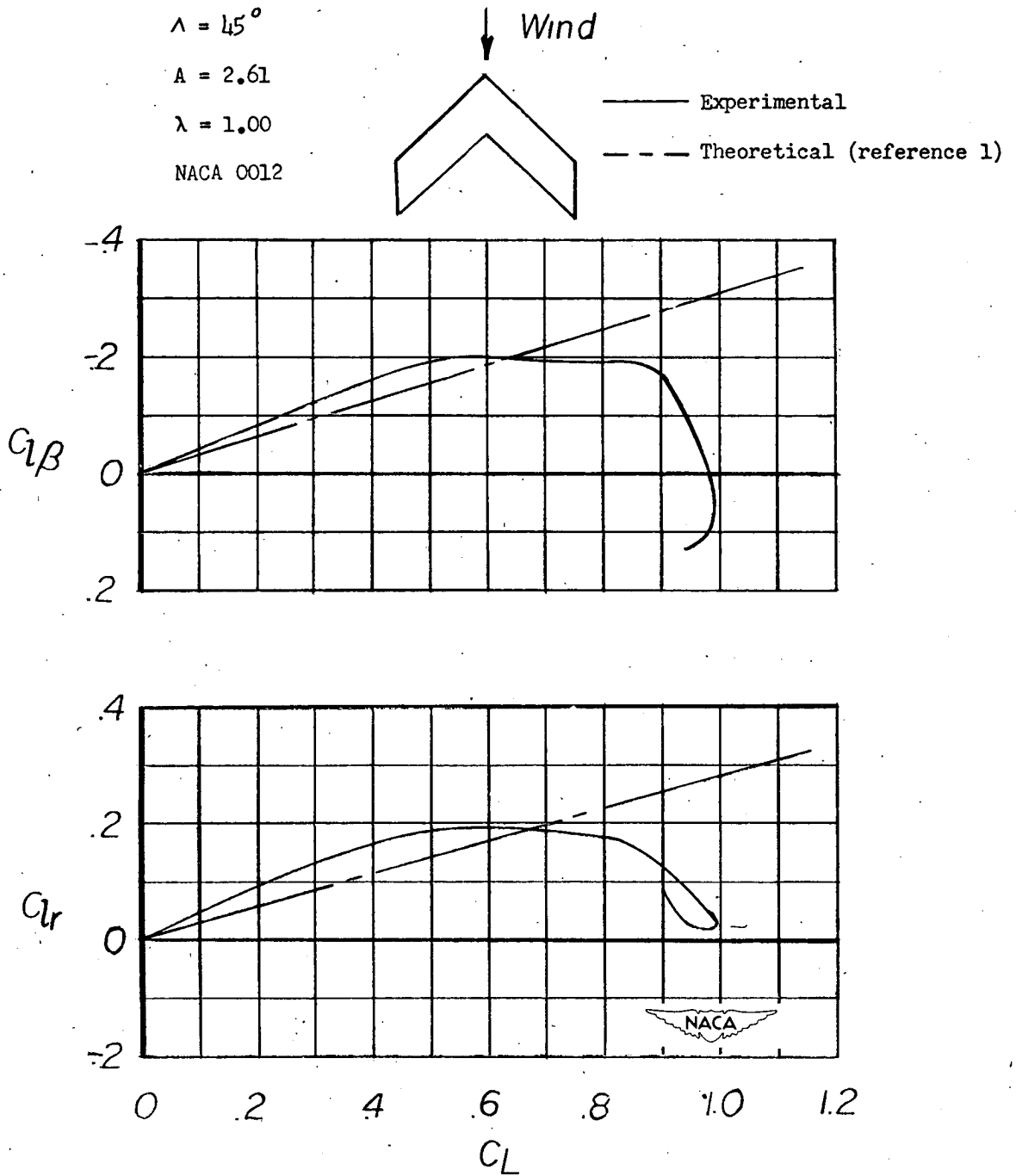


Figure 1.- Variation of  $C_{l_{\beta}}$  and  $C_{l_r}$  with lift coefficient for a  $45^\circ$  sweptback wing.

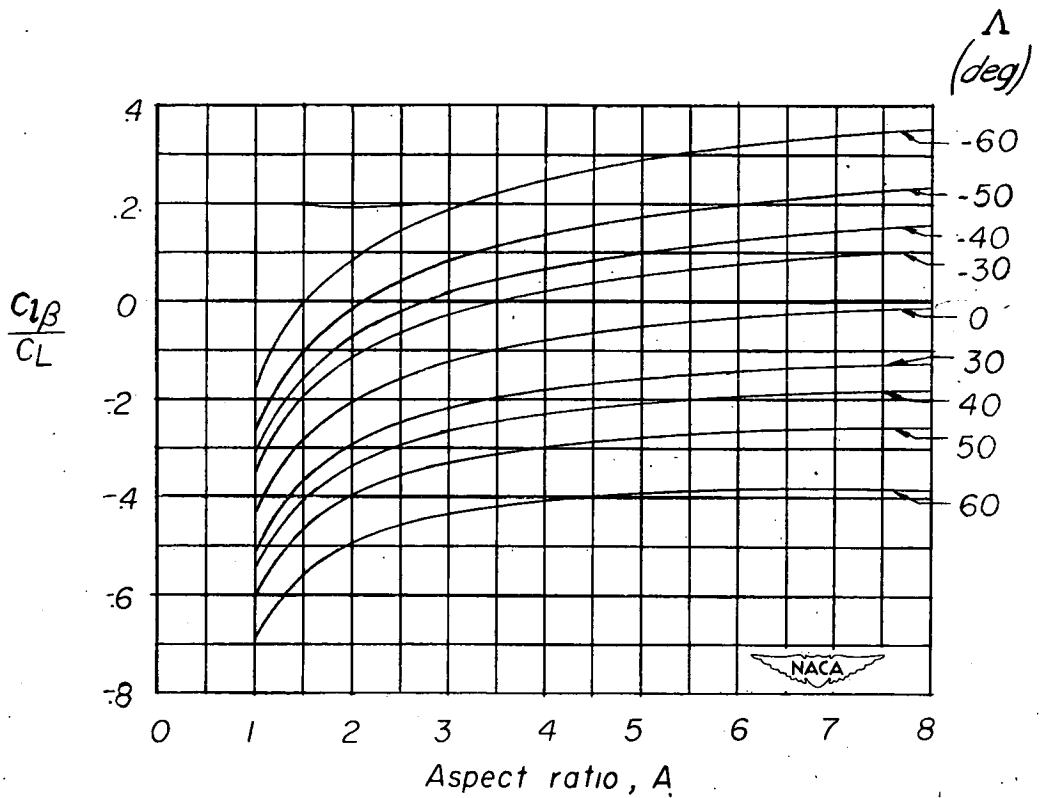


Figure 2.- Variation of the rolling moment due to sideslip with aspect ratio for various sweep angles.  $a_0 = 5.67$ ;  $\lambda = 1.0$ . (Reference 1)

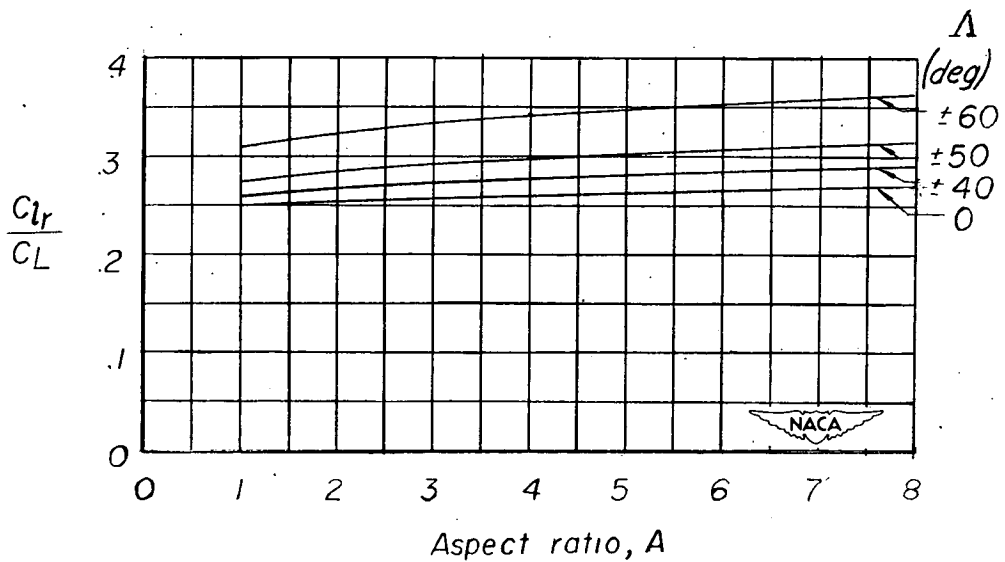


Figure 3.- Variation of the rolling moment due to yawing with aspect ratio for various sweep angles.  $\lambda = 1.0$ ;  $\frac{\bar{x}}{c} = 0$ . (Reference 1)



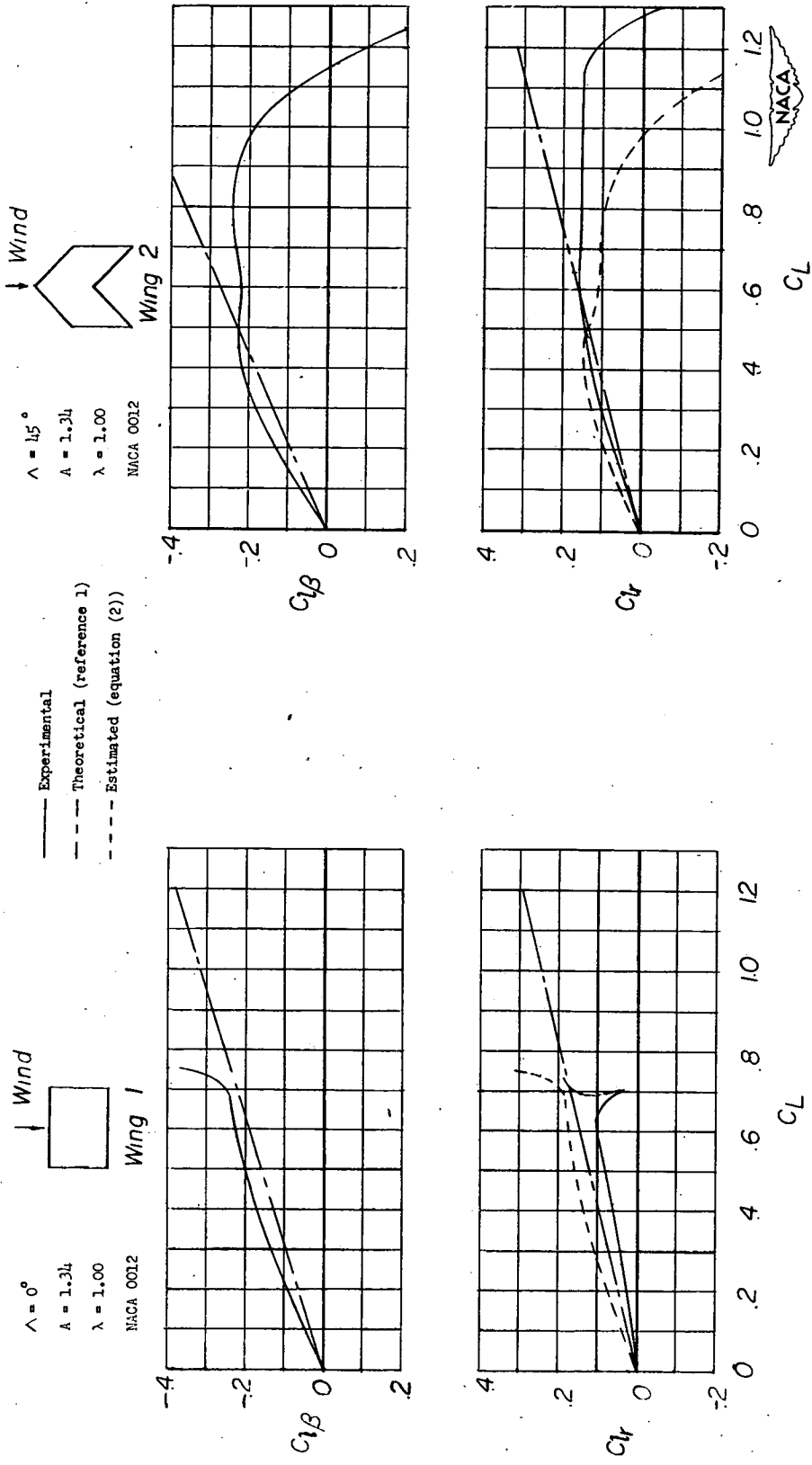


Figure 4.- Estimation of the rolling moment due to yawing for wings 1 and 2.

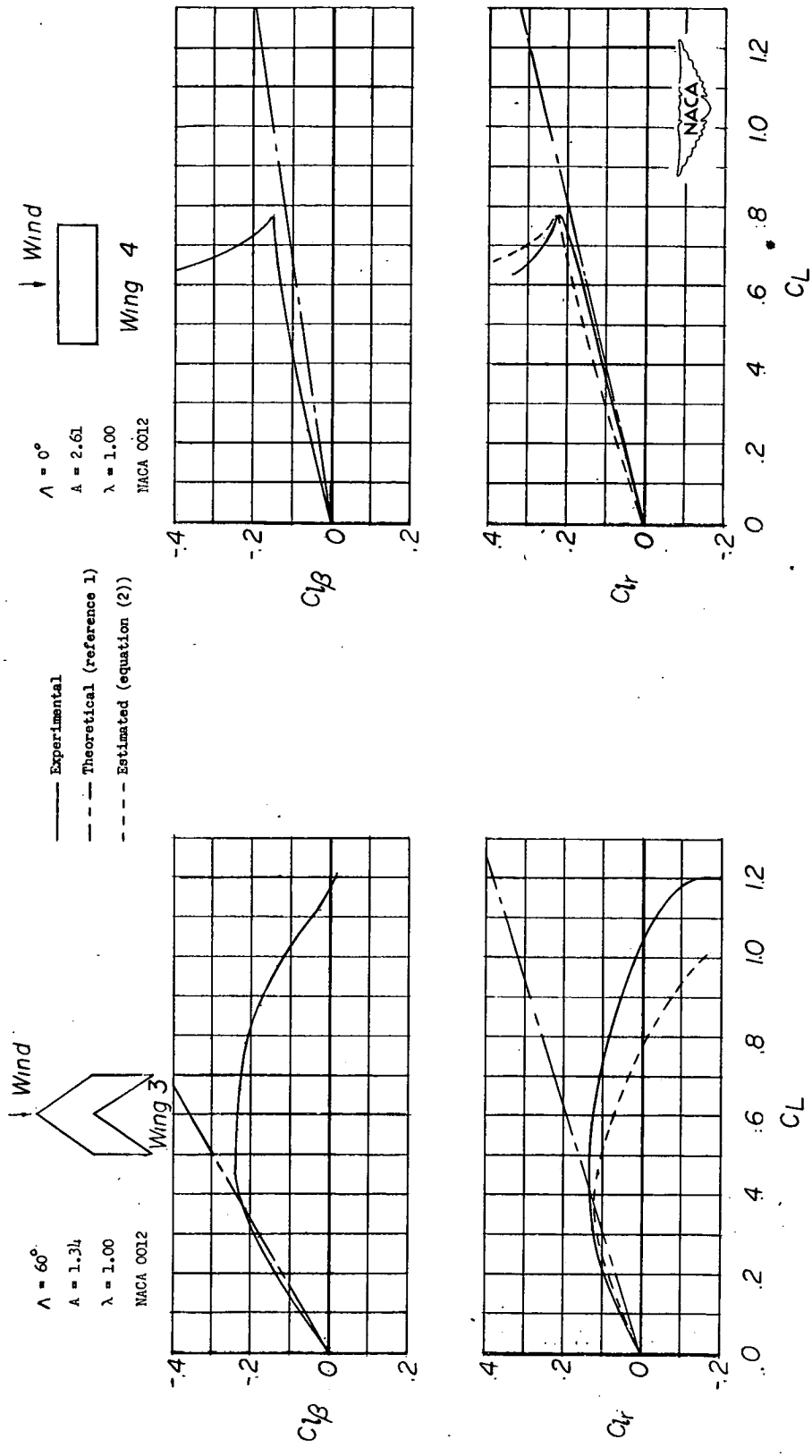


Figure 5.- Estimation of the rolling moment due to yawing for wings 3 and 4.

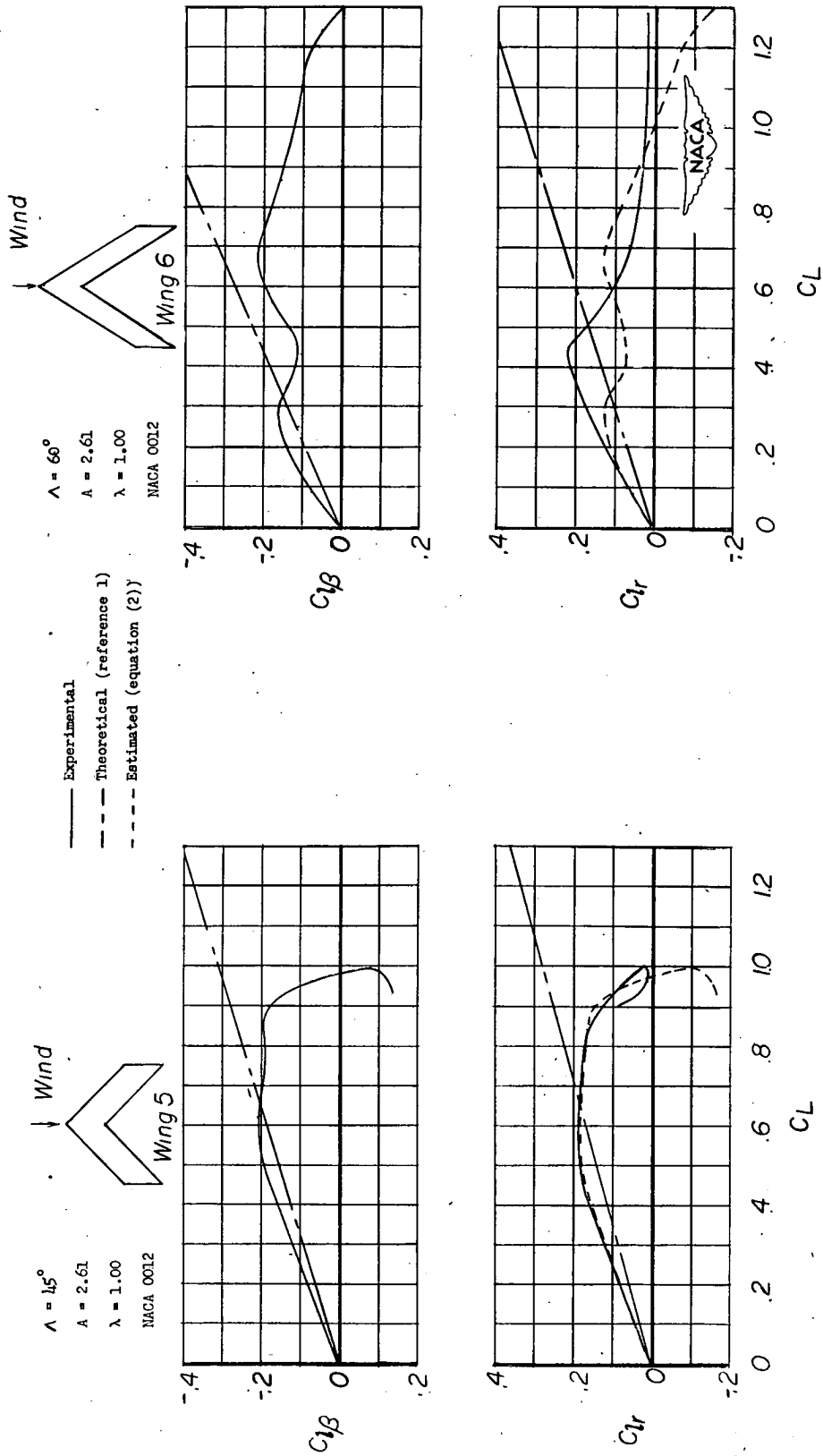


Figure 6.- Estimation of the rolling moment due to yawing for wings 5 and 6.

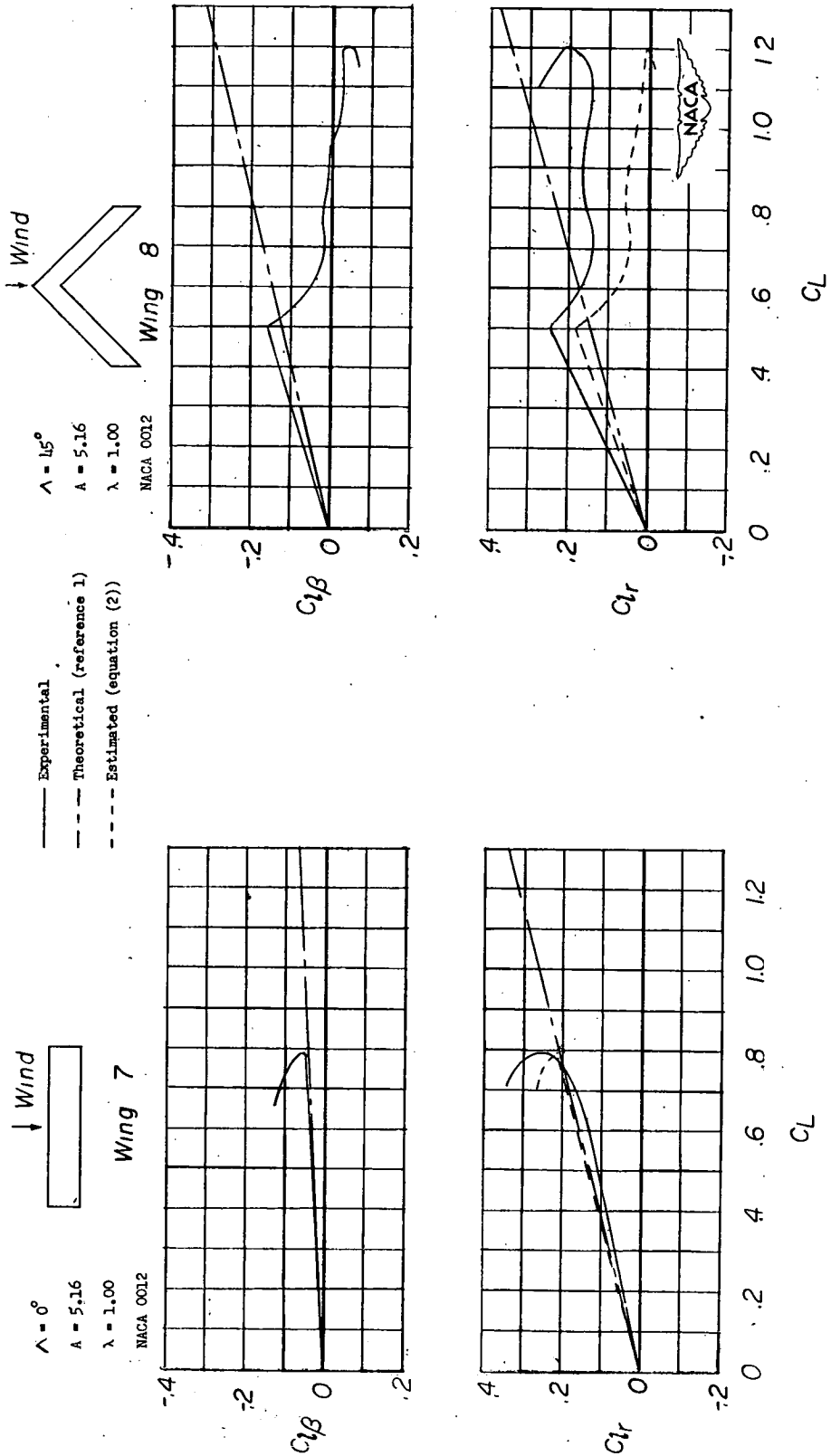


Figure 7.- Estimation of the rolling moment due to yawing for wings 7 and 8.

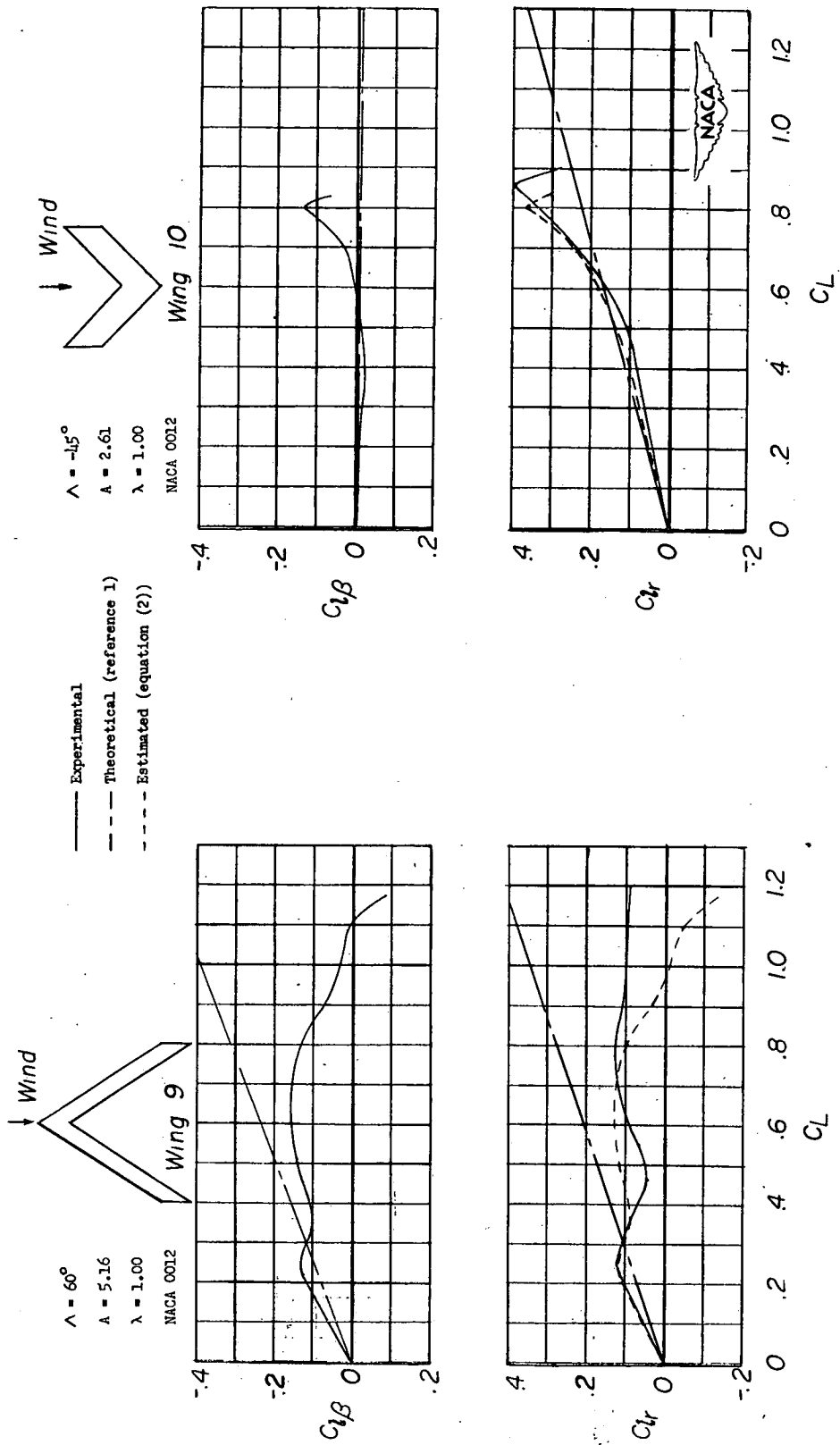


Figure 8.- Estimation of the rolling moment due to yawing for wings 9 and 10.

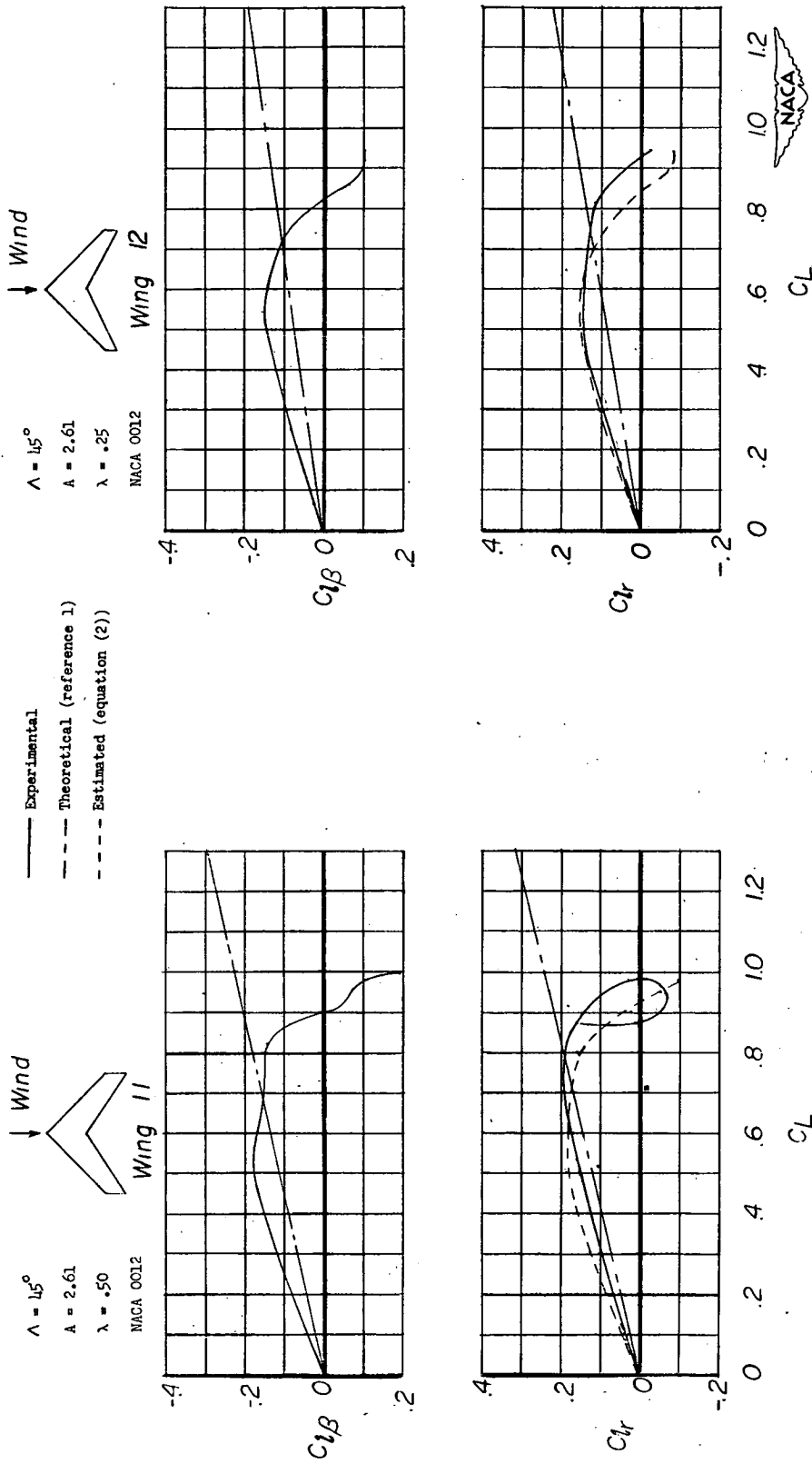


Figure 9.- Estimation of the rolling moment due to yawing for wings 11 and 12.

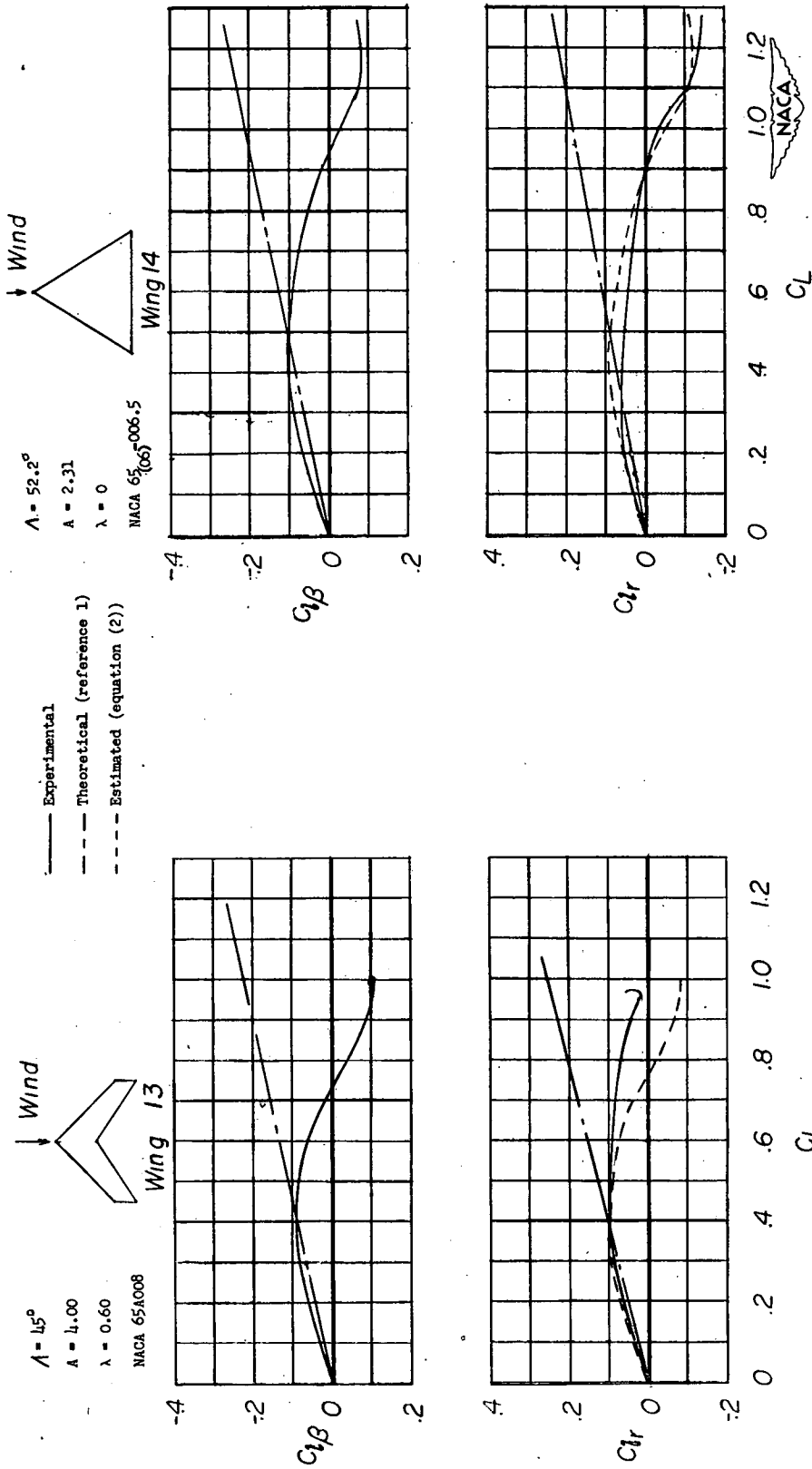


Figure 10.- Estimation of the rolling moment due to yawing for wings 13 and 14.

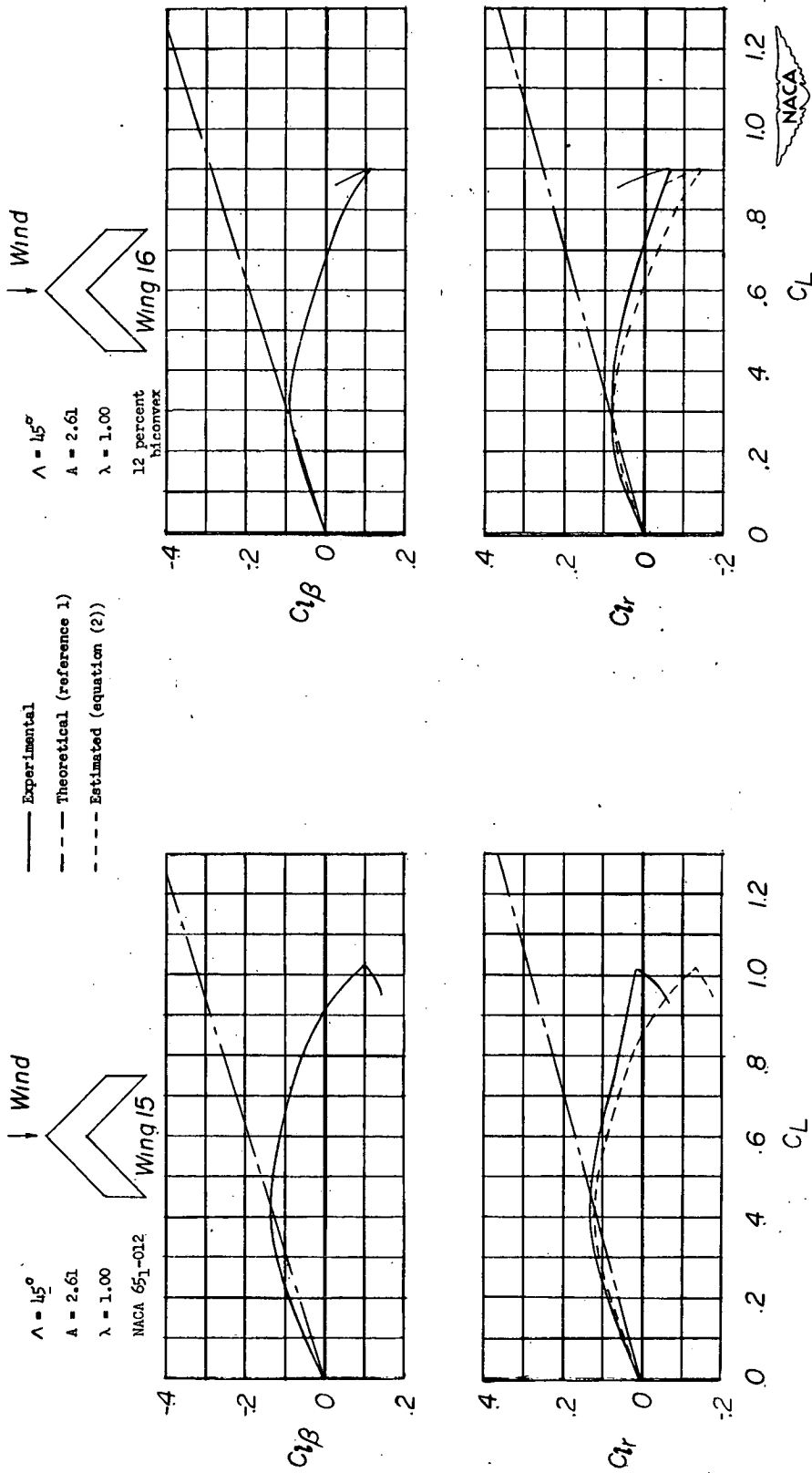


Figure 11.- Estimation of the rolling moment due to yawing for wings 15 and 16.



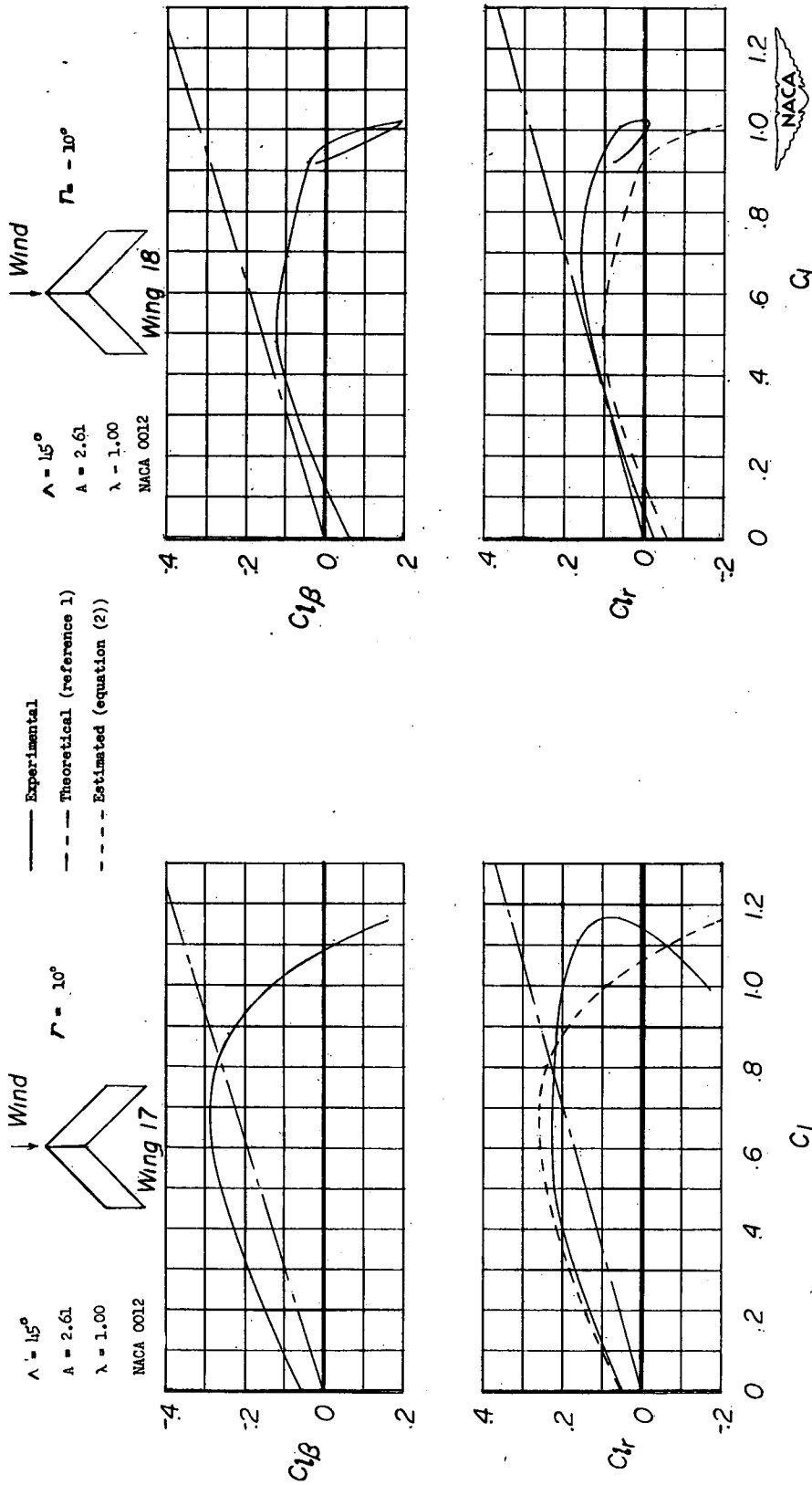


Figure 12.- Estimation of the rolling moment due to yawing for wings 17 and 18.

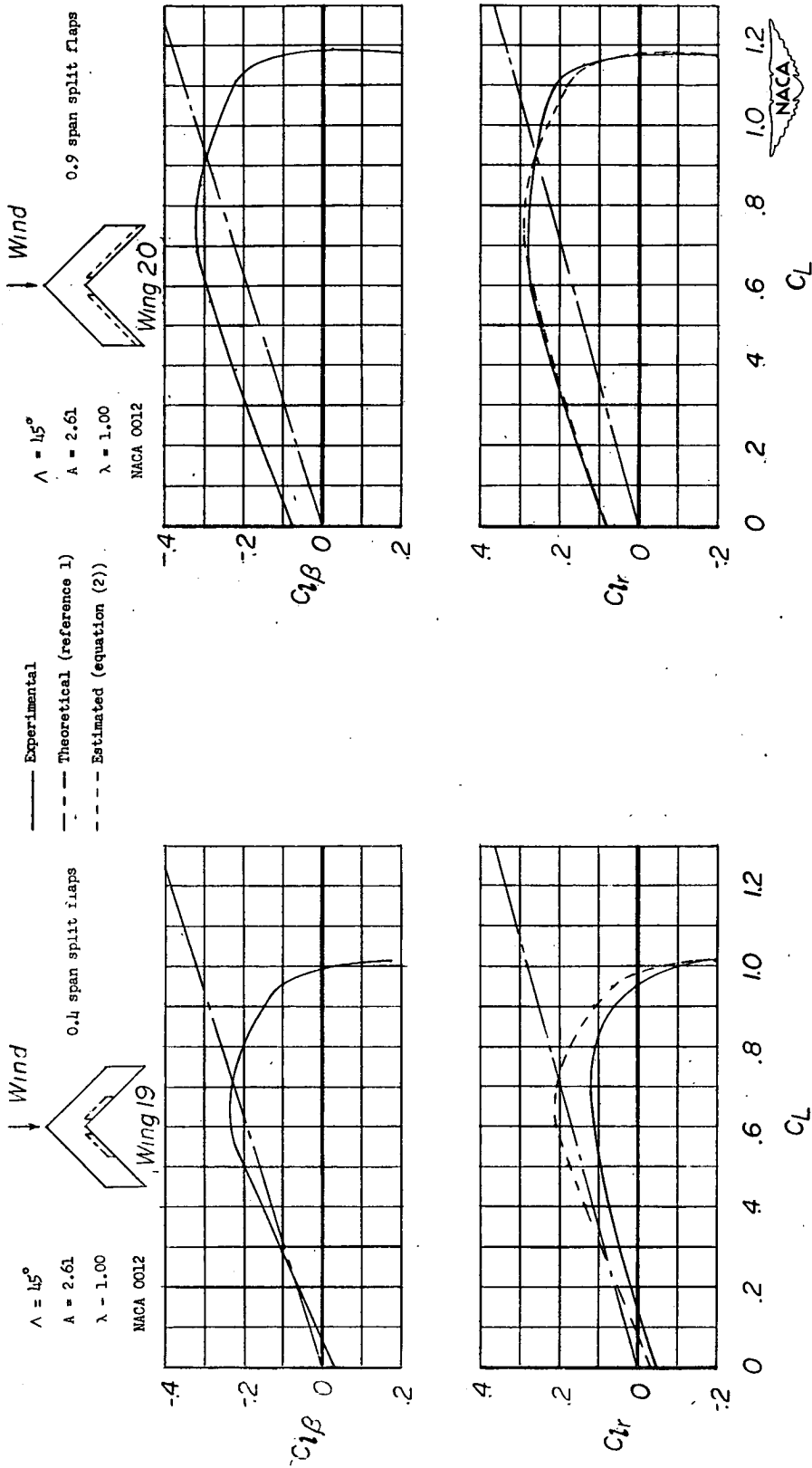


Figure 13.- Estimation of the rolling moment due to yawing for wings 19 and 20.

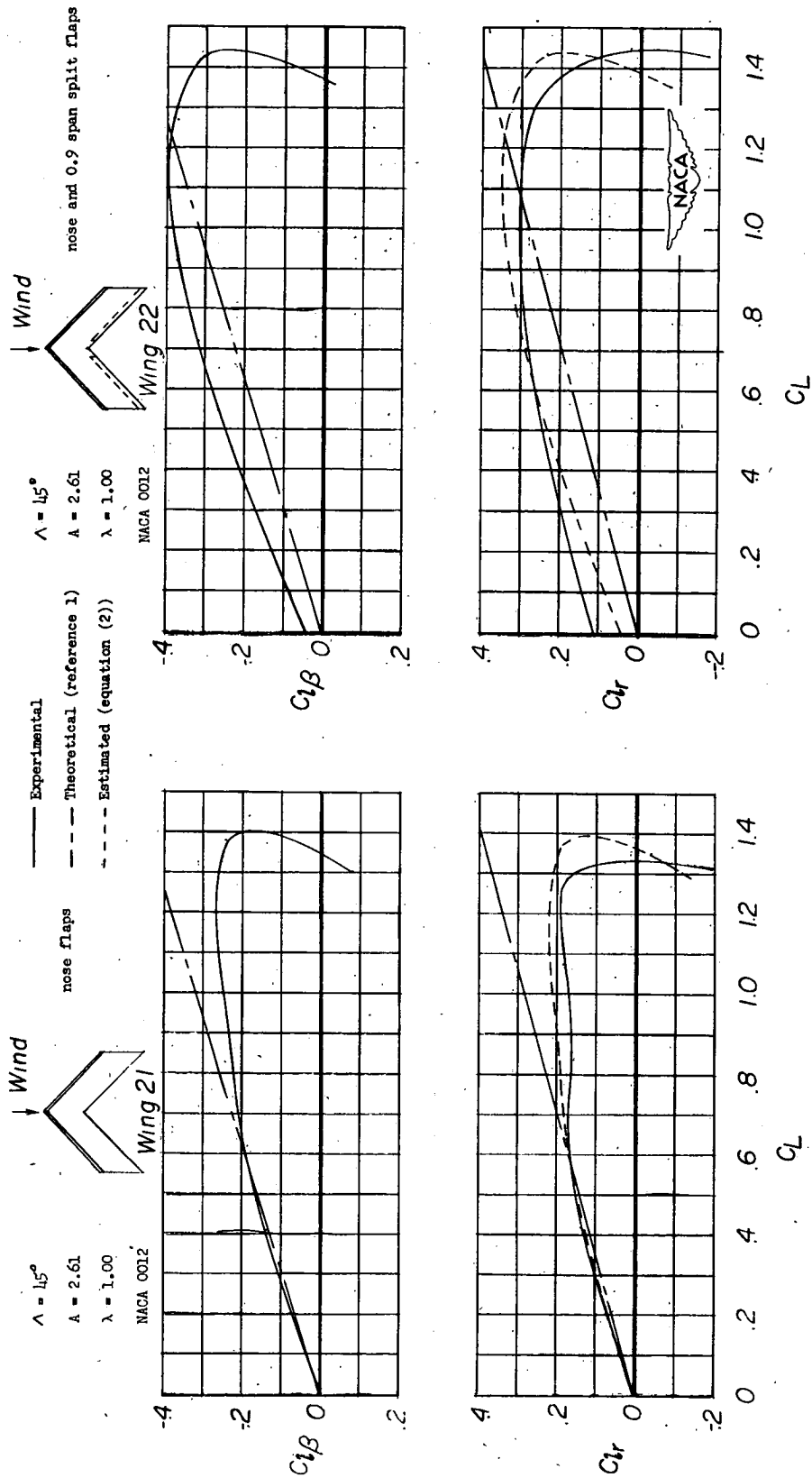


Figure 14.- Estimation of the rolling moment due to yawing for wings 21 and 22.

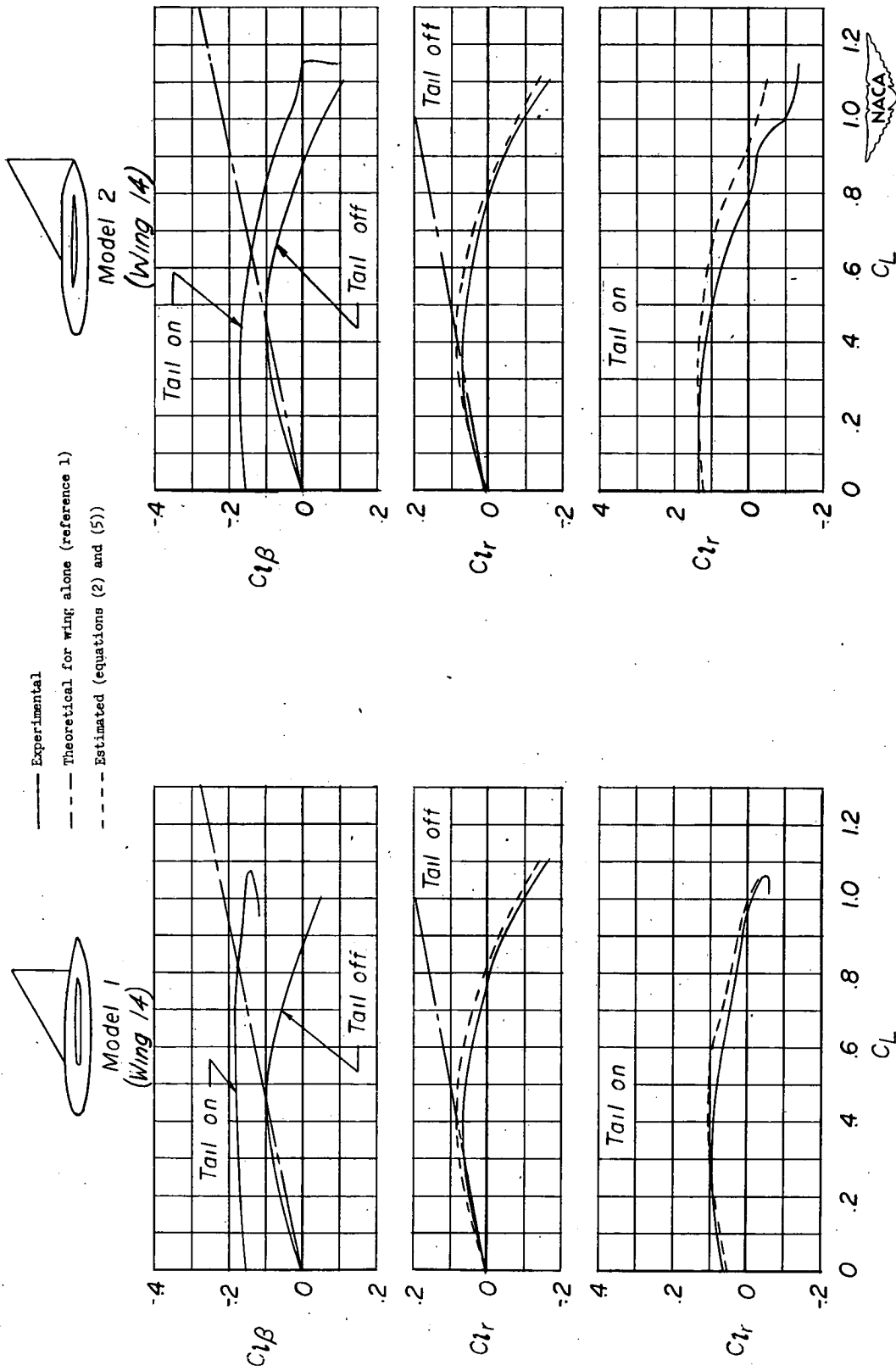


Figure 15.- Estimation of the rolling moment due to yawing for models 1 and 2.

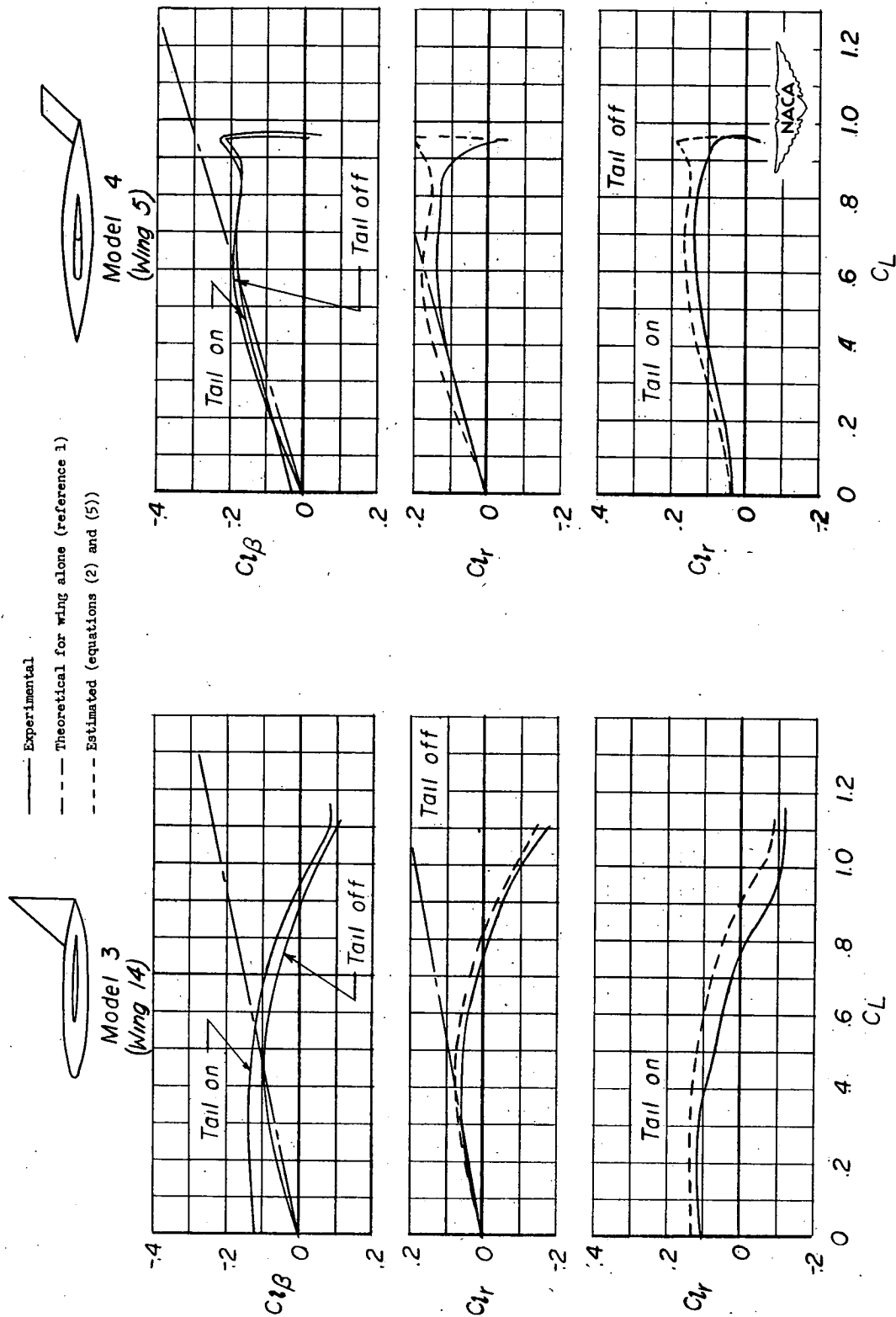


Figure 16.- Estimation of the rolling moment due to yawing for models 3 and 4.

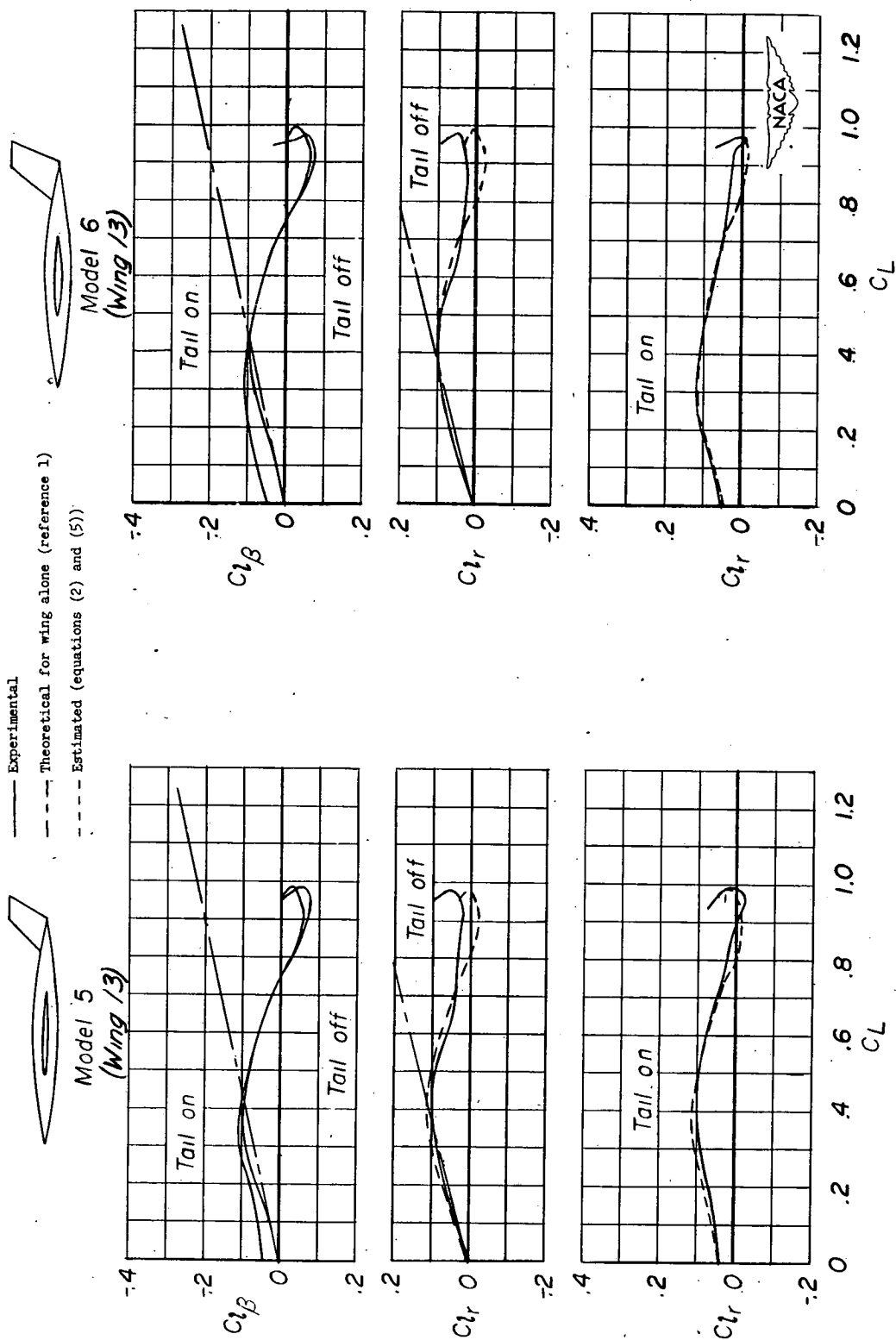


Figure 17.- Estimation of the rolling moment due to yawing for models 5 and 6.

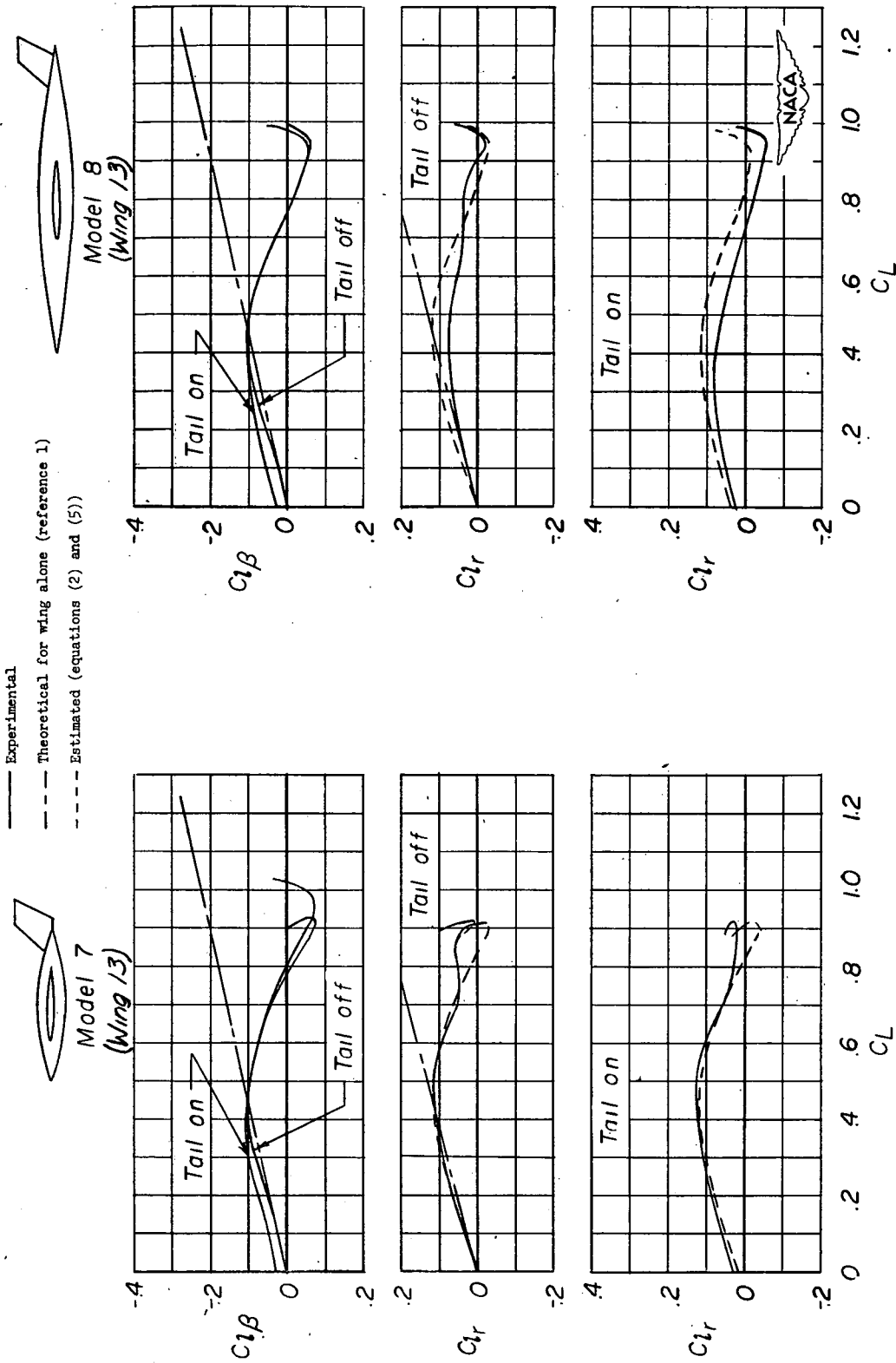


Figure 18.- Estimation of the rolling moment due to yawing for models 7 and 8.